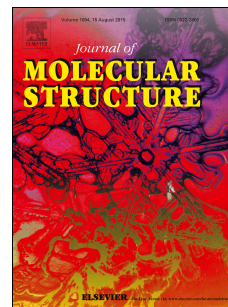


Accepted Manuscript

Fluorescent triazolyl spirooxazolidines: Synthesis and NMR stereochemical studies

Patryk Kasza, Marcela E. Trybula, Katarzyna Baradziej, Mariusz Kepczynski,
Przemysław W. Szafranski, Marek T. Cegła



PII: S0022-2860(19)30062-6

DOI: <https://doi.org/10.1016/j.molstruc.2019.01.052>

Reference: MOLSTR 26103

To appear in: *Journal of Molecular Structure*

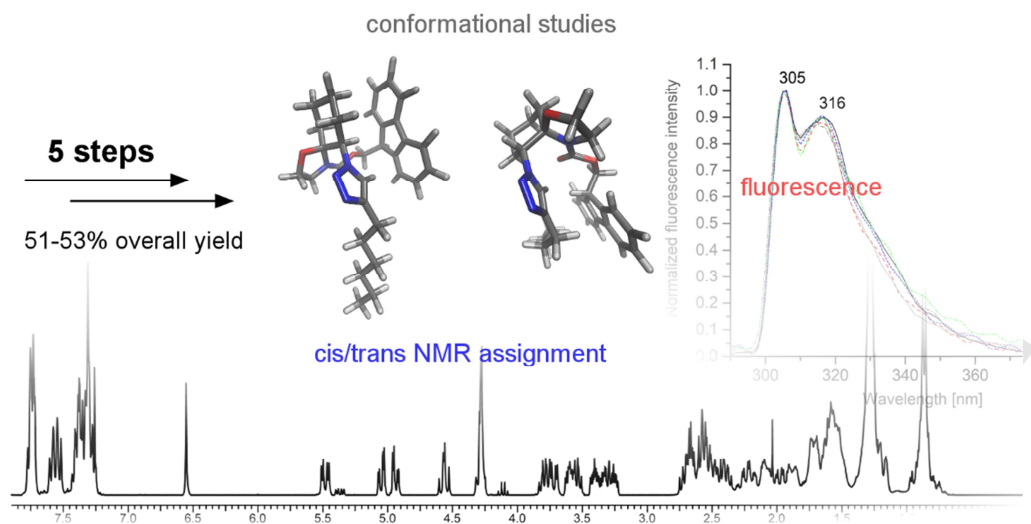
Received Date: 3 October 2018

Revised Date: 20 December 2018

Accepted Date: 14 January 2019

Please cite this article as: P. Kasza, M.E. Trybula, K. Baradziej, M. Kepczynski, Przemysław W. Szafranski, M.T. Cegła, Fluorescent triazolyl spirooxazolidines: Synthesis and NMR stereochemical studies, *Journal of Molecular Structure* (2019), doi: <https://doi.org/10.1016/j.molstruc.2019.01.052>.

This is a PDF file of an unedited manuscript that has been accepted for publication. As a service to our customers we are providing this early version of the manuscript. The manuscript will undergo copyediting, typesetting, and review of the resulting proof before it is published in its final form. Please note that during the production process errors may be discovered which could affect the content, and all legal disclaimers that apply to the journal pertain.



Fluorescent triazolyl spirooxazolidines: synthesis and NMR stereochemical studies

Patryk Kasza,^a Marcela E. Trybula,^{b,c} Katarzyna Baradziej,^a Mariusz Kepczynski,^d Przemysław W. Szafranski,^{*a} and Marek T. Cegła^a

*p.szafranski@uj.edu.pl

^aDepartment of Organic Chemistry, Faculty of Pharmacy, Jagiellonian University Medical College, Medyczna 9 st. 30-688 Kraków, Poland.

^bDepartment of Multilayer Materials, Institute of Metallurgy and Materials Science, Polish Academy of Sciences, Reymonta 25 st., 30-688 Kraków, Poland.

^cDepartment of Materials Science and Engineering KTH Royal Institute Technology Brinellvägen 23, SE-100 44 Stockholm, Sweden.

^dDepartment of Physical Chemistry, Faculty of Chemistry, Gronostajowa 2 st., 30-387 Kraków, Poland

Abstract

Carbon-heteroatom chemistry is a method of choice for rapid construction of complex molecules. In the recent decade, its various applications flourished thanks to the Click chemistry approach. Herein, we use a combination of C-X formation reactions to complete the synthesis of 1,2,3-triazolyl spirooxazolidines, bearing the fluorenylmethoxycarbonyl (fmoc) substituent. Thanks to the application of 2D-NMR spectroscopic methods and a multilevel computational approach, including a medicinal chemistry – inspired conformational search, PM7 semiempirical and DFT-based geometry optimization finalized with DFT-GIAO NMR shielding constant calculation, we were able to investigate the conformational space and assign cis/trans configuration in complex NMR spectra. For the obtained fmoc derivatives we recorded UV-VIS absorption and emission spectra. The obtained compounds contain pharmacophoric groups characteristic for endocannabinoid system modulators-CB1 receptor ligands or FAAH inhibitors.

Keywords:

Triazole, oxazolidine, spirooxazolidine, NMR, stereochemistry

Introduction

Rapid construction and detailed investigation of complex spirocyclic structures has been a proving ground for synthetic methodologies and a theme of recent interesting findings.¹⁻³ An efficient way to obtain such architectures is through carbon-heteroatom chemistry. In the last decade, the *click chemistry* concept, based on C-X bond formation,⁴ has conquered numerous research fields, such as materials and medicinal chemistry,⁵⁻¹¹ promoting the copper-catalyzed azide-alkyne cycloaddition (CuAAC).¹² In contrast, the efficient heterocycle formation reactions, based on carbonyl chemistry, are seldom associated with *click chemistry*, even though they found place in the seminal article by Sharpless et al. (“carbonyl chemistry of non-aldol type”).⁴ An interesting example is the synthesis of 1,4-oxaaza [4.5] spirodecane (spirooxazolidine) systems from ethanolamine and cyclic ketones, first demonstrated by Cope et al.^{13,14} Despite the long history, relatively few such compounds are known in the literature, probably due to instability in acidic conditions and complex stereochemistry. However, some of the recent contributions include NMR stereochemical studies on oxazolidines, diazolidines and dioxolidines¹⁵. These investigations concerned synthesis and antimicrobial studies of substituted 1,4-oxaaza [4.5]spirodecanes, and their thiourea derivatives, active against *Staphylococcus* and *E. coli*,¹⁶ or biological activity studies of sulfonylurea oxazolidine derivatives.¹⁷

Ethanolamine, the building block for oxazolidine construction, is a small molecule of considerable physiological significance. It is necessary for the synthesis of endogenous cannabinoid receptor ligands such as anandamide, virodhamine¹⁸ or N-palmitoyl ethanolamine¹⁹. Introduction of this fragment into triazole-based molecular architectures investigated in our laboratory in the context of CB1 receptor affinity or fatty acid amide hydrolase (FAAH) inhibition^{20,21}. It is also important for synthetic methodology, medicinal chemistry and structural space for further research.

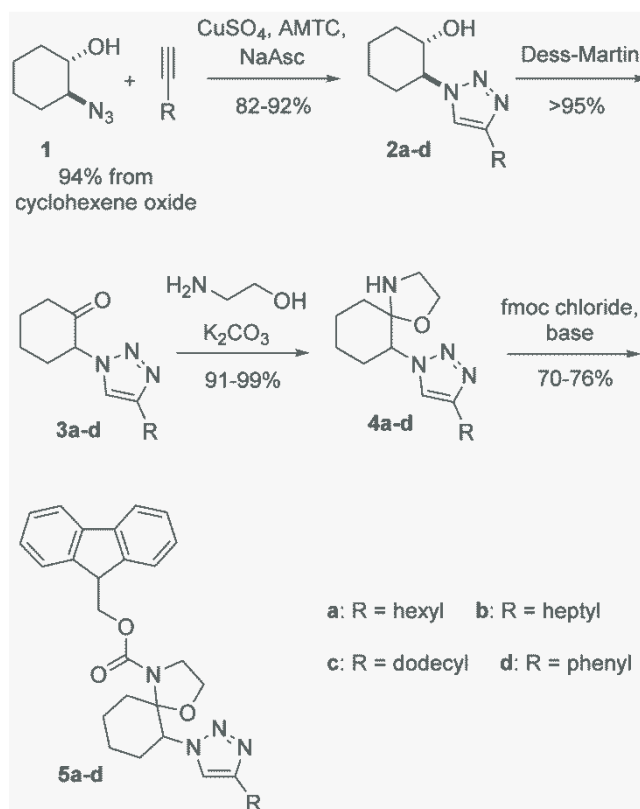
Herein, we present an efficient combination of several click chemistry reactions, including CuAAC and carbonyl-based oxazolidine formation, to complete the synthesis of novel 1,2,3-triazolyl spirooxazolidine derivatives in four steps. In one further step, we introduce the fluorenylmethoxycarbonyl (fmoc) fragment, which makes spirooxazolidines resistant to acidic environment and introduces fluorescent properties.²²⁻²⁴ The fmoc fragment is an amine-protecting group, widely used in peptide synthesis. A review concerning the use of fmoc-aminoacids and short peptides in functional material synthesis has been published recently by Tao and coworkers²⁵. Apart from peptide synthesis, the fmoc fragment has also found application in the construction of complex natural product structures such as Saframycin²⁶. In 2017 Lypson and Wilcox used the fmoc, protecting group as a synthetic tool, in a study on β -turn mimetics, however it was eliminated from the final compounds to simplify the structure and NMR spectra²⁷.

The synthetic pathway presented herein is an example of introducing the ethanolamine moiety into the structures of triazole derivatives, while the obtained compounds exhibit interesting structural and conformational features. This may lead to new classes of CB1 receptor ligands of FAAH inhibitors. We describe the development of synthetic procedure, conformational studies and NMR assignment using an efficient combination of 2D NMR spectroscopy and computational methods. This allowed to investigate the influence of triazolyl and fluorenyl ring currents on NMR spectra of the spirocyclic system and assign relative stereochemistry in complex diastereoisomeric mixtures. The UV-VIS absorption and emission spectra of the final fluorenyl derivatives are also presented.

Results and discussion

Synthesis

The synthetic route we developed is shown in Scheme 1; the synthesis of *trans*-2-azidocyclohexanol **1** from epoxycyclohexane was omitted. Triazolyl cyclohexanols **2** were obtained through cycloaddition of **1** with appropriate commercially available alkynes and oxidized to ketones **3**, which were subsequently reacted with ethanolamine. Finally, the spirooxazolidines **4** were acylated with fmoc-chloride to obtain the fluorescent amide derivatives **5**.



Scheme 1: Synthesis of oxazolidines **4** and their fmoc derivatives **5**

Trans-2-azidocyclohexanol **1** was prepared from epoxycyclohexane in 94% yield, using a modified literature method.²⁸ The cycloadditions of **1** with 1-octyne, 1-nonyne, 1-tetradecyne and phenylacetylene were carried out with 0.5 - 5mol% of copper and 1 - 10mol% AMTC ligand, according to a protocol developed in our laboratory.²⁹ In the case of triazole **2c**, only 0.5 mol% Cu was sufficient to achieve over 90% yield.

Oxidation of the triazolyl alcohols **2a-d** was completed in nearly quantitative yields using the Dess-Martin periodinane. The alcohols could be oxidized with the Jones reagent or a modification of the Swern oxidation, using tosyl chloride as DMSO activator in low to moderate yields. In search of a cheaper and more “green” protocol, several other methods have been tested unsuccessfully, including the Cornforth and Stevens oxidation, tert-butyl hydroperoxide or hydrogen peroxide and Cu(II) complexes. Such resistance to oxidation could result from the presence of a strong intramolecular hydrogen bond between the hydroxyl proton and the N2 nitrogen of the triazole ring. This bond can be particularly short (<1.5 Å) and closes a six-membered ring. For alcohol **2a**, this could be confirmed by the presence of CH-OH coupling ($J = 3.78$ Hz),³⁰ caused by blocked hydroxyl group rotation. Efficient alcohol oxidation established the advantage over an alternative synthetic pathway through 2-azidocyclohexanone.³¹⁻³⁴

The key step of the synthetic pathway was formation of the spirocyclic fragment. Ketones **3** were reacted with excess ethanolamine and K_2CO_3 as a base facilitating the ring closure. The reactions were completed after one hour at 110°C and ¹H NMR spectra showed the presence of both *cis* and *trans* oxazolidine **4** diastereoisomers at a roughly equimolar ratio. They were unstable under acidic conditions: no M+1 ions were recorded in LC-MS measurement using 0.5% HCOOH eluent.

Introduction of the fmoc fragment to obtain the amide derivatives **5 a-d** was relatively straightforward, but care was required due to the acid-sensitivity of the spirooxazolidine substrates (**4**). A simple

procedure using fmoc chloride and K_2CO_3 in dichloromethane furnished the amides **5** in 70-76% yield. The products contained small amounts of ketones **3** resulting from substrate decomposition. Variations of the procedure using less acidic fmoc succinimidyl ester (fmoc-OSu) or different bases were unsuccessful.

Conformational studies

To understand the structure of spirooxazolidine derivatives **4** and **5**, and to facilitate the assignment of NMR signals, computational studies were performed for compounds **4a**, **5a** and **5d**. Large conformation sets were generated using a genetic-algorithm-based approach^{35,36} and optimized using the PM7 semiempirical method (the Balloon program).^{37,38} Selected best conformations were re-optimized using DFT (B3LYP functional and 6-31G(d,p) basis). Subsequently, Boltzmann distribution was calculated and the conformations that represented >95% total occupancy were used for DFT-GIAO NMR shielding constant calculation (CAMB3LYP, cc-pvtz basis).³⁹ Semiempirical and DFT calculations for the conformational search and shielding constant calculation were performed using continuum solvent models⁴⁰ (COSMO for PM7 and IEFPCM for DFT). Top conformations for all the investigated compounds are shown in Figure 1; the procedure is described in the experimental section. Additional data, including more figures, top conformer coordinates with energies and shielding constant values, are available in the electronic supporting information.

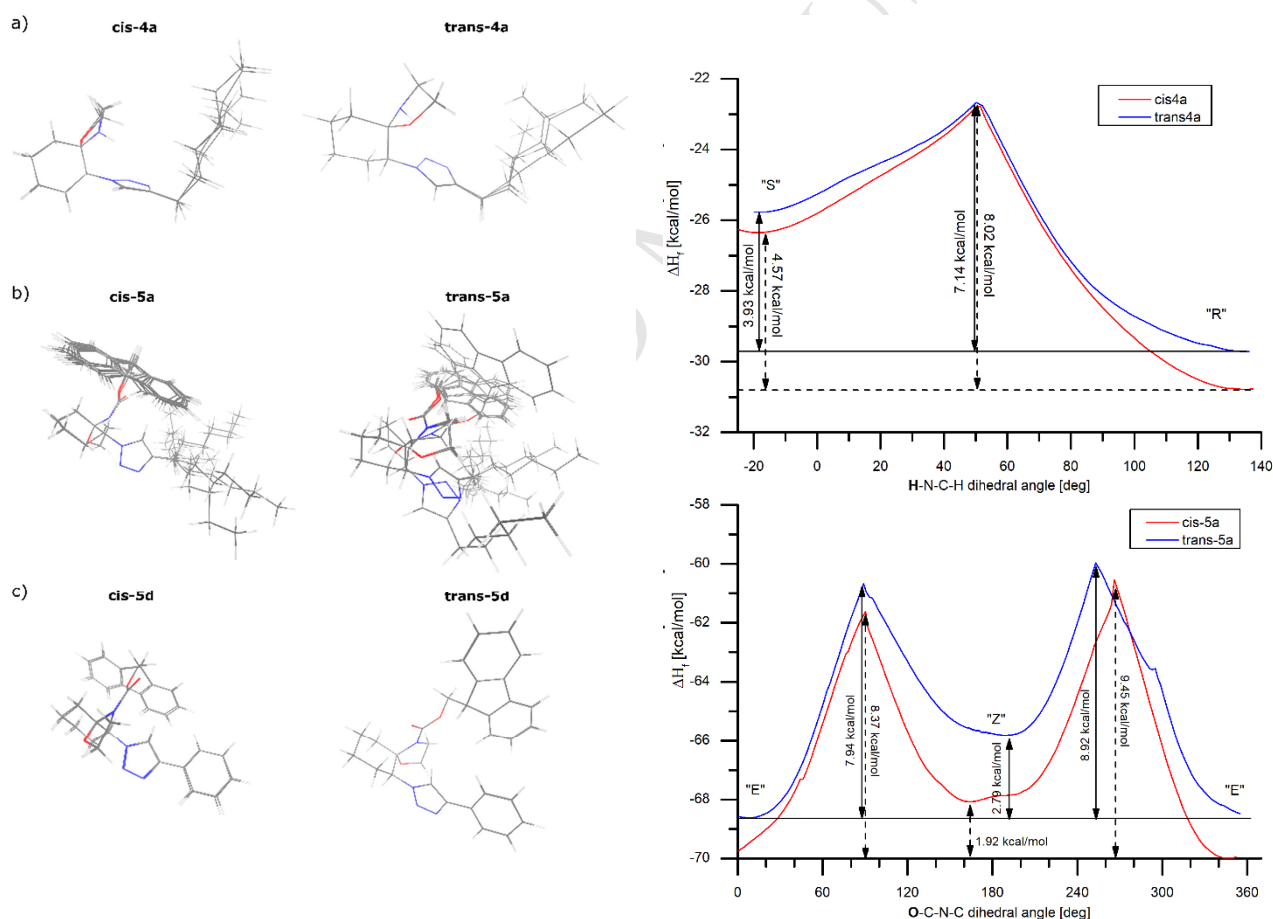


Figure 1 (left). Lowest-energy conformations taken for NMR shielding constant calculation: a) *cis* and *trans* **4a**, b) *cis* and *trans* **5a**, c) *cis* and *trans* **5d**

Figure 2 (right). Top panel: rotation barriers for nitrogen inversion, calculated for *cis-4a* and *trans-4a*; bottom panel: rotation barriers for the amide bond in *cis-5a* and *trans-5a*.

For **5a** and **5d**, introduction of the fmoc fragment resulted in expanding the conformational space and introduced significant changes in the NMR spectra due to the large and strong aromatic ring current. For *cis-5a* and *cis-5d* the fluorenyl fragment folds towards the cyclohexyl ring, whereas for *trans-5a* it adopts a number of positions with a general outward preference. For *trans-5d*, this conformational diversity was reduced down to small variations of one conformation with an outward-facing fluorenyl. Identification of these phenomena facilitated distinguishing between *cis* and *trans* signals.

The conformation generation procedure is constructed in a manner that conserves geometric configuration on nitrogen atoms where nitrogen-inversion is possible. Therefore, it was important to determine which conformers display lower energy and whether the nitrogen-inversion atropoisomerism is possible for the studied system. To do that, conformational analysis was performed for the H-N-C-H dihedral angle in the oxazolidine ring which would change upon nitrogen flip. For that purpose, a reaction path was calculated using the PM7 method in MOPAC, with the H-N-C-H angle as coordinate and 2° step. As starting points, top conformations (as determined using the PM7 method) were taken for each diastereoisomer. The result, plotted in Figure 2 (top panel), clearly showed that no atropoisomerism can be expected, as the estimated energy barrier was around 8 kcal/mol for both diastereoisomers. The “R” isomer of *cis* and *trans 4a*, where the amine proton is directed towards the triazole ring, was energetically favorable (Figure 2, top). To confirm that, a larger set of conformations was tested with overall prevalence of the “R” conformers over “S”. An analogous study was performed for E/Z isomerism of the amide bond in compound **5a** (Figure 2, bottom panel). In this case the energy barriers are also close to 8 kcal/mol, which indicates free rotation. The “E” conformers were energetically favorable, however in the case of amide bond the Balloon-generated conformation sets contained all of its geometric variants. In both cases (**4a** and **5a**) the computational results, showing free rotation, are consistent with the experimental data, where no hints of atropoisomerism could be observed.

NMR spectra

The NMR spectra of diastereoisomeric mixtures, obtained for **4** and **5**, were complex and required a combination of several experimental and computational methods to correctly assign the signals. The assignment proceeded in two steps: first the signals were assigned to respective structural fragments using COSY and HSQC spectra; labeled excerpts from HSQC spectra shown in Figures 3-5 b). Next, the data were compared to the chemical shifts computed using the DFT-GIAO method. The computational results are shown in Figures 3-5 c). The discrepancies between experimental and computed chemical shifts were larger than those usually observed for similar methodology applied to smaller and less complex structures. Three significant factors could contribute to this situation: structural complexity combined with conformational freedom of the investigated compounds, large influence of the ring currents, and possible *cis-trans* complex formation (discussed further). The first two factors limited the basis set size, as the addition of disperse functions resulted in severe convergence problems, probably due to the intramolecular interactions. Therefore the assignment of NMR signals relied on finding the trends resulting from ring current influence reproduced in the conformations found. The comparison to 2D-NMR HSQC spectra was crucial to locate the diastereotopic protons in the heavily overlaid 1D NMR spectrum and enable a proper comparison with computational data.

The ¹H NMR and HSQC spectra together with computational results and proton assignment for compounds **4a**, **5a** and **5d** are shown in Figures 3 – 5, respectively. For compound **4a**, protons **a** and **b** in the *cis* isomer are shifted downfield from respective *trans*- protons. In *cis-4a*, both **c** and **d** protons are diastereotopic with a chemical shift difference between **c** and **c'** or **d** and **d'** around 0.5 ppm. In contrast, for *trans-4a*, **D** and **D'** protons are only slightly separated (~0.2 ppm), whereas for **C** and **C'**—the difference in chemical shift is over 1 ppm. These differences result from positioning of the spirooxazolidine system relative to the triazole ring.

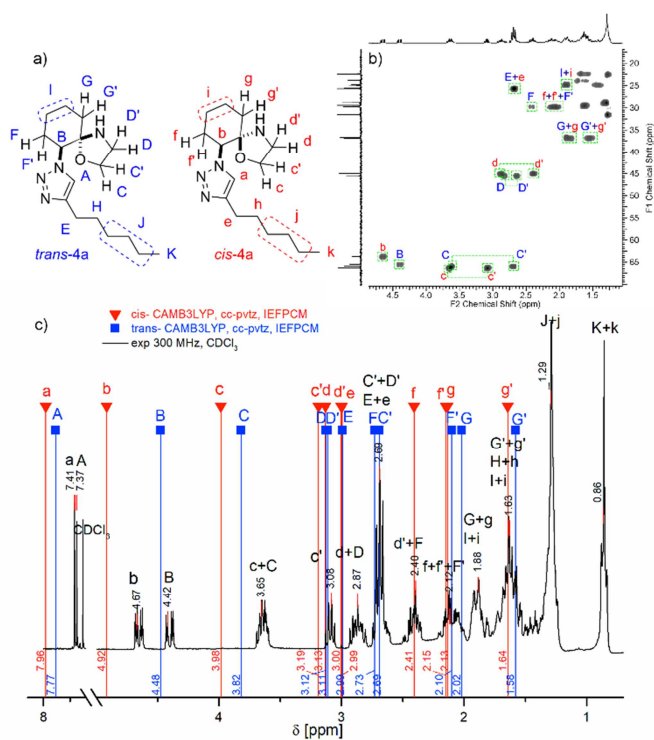


Figure 3. NMR results for **4a**: a) chemical structures, b) HSQC spectrum with assignment c) HNMR spectrum with selected computational results.

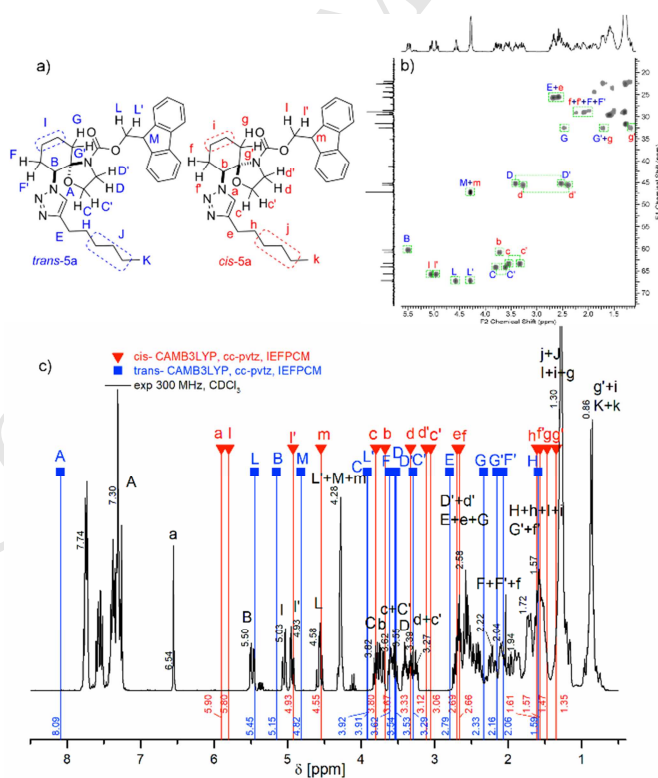


Figure 4. NMR results for **5a**: a) chemical structures, b) HSQC spectrum with assignment c) HNMR spectrum with selected computational results

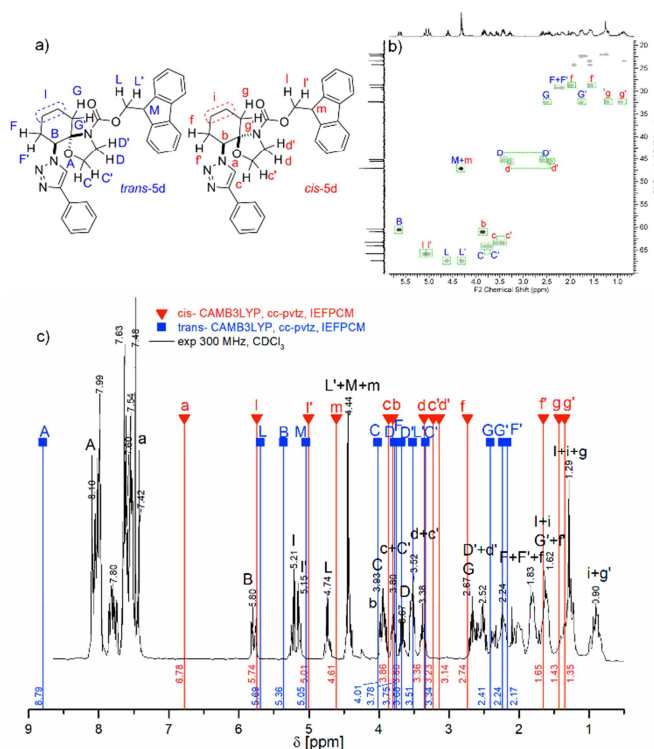


Figure 5. NMR results for **5d**: a) chemical structures, b) HSQC spectrum with assignment c) HNMR spectrum with selected computational results

In *cis*-**4a**, the triazole and oxazolidine rings are closer, with both methylene groups (NCH_2 and OCH_2) above the aromatic ring plane and **b** proton almost parallel to it. Therefore, **c'** and **d'** protons are found under the influence of the triazole ring current causing an upfield shift, while **c** and **d** protons facing away from the triazole are shifted downfield. In *trans*-**4a**, only the OCH_2 fragment is situated directly above the triazole, which causes a large upfield shift of **C'** proton relatively to the outward facing **C** proton. At the same time the NCH_2 group in *trans*-**4a** is shifted outward, with **D** and **D'** protons removed from the ring current. The **B** proton is perpendicular to the aromatic ring plane. For compounds **5a** and **5d**, introduction of the fmoc fragment significantly changed the NMR spectra. The most spectacular change was in the chemical shifts of axial protons **b** and **I** in the cyclohexyl fragment. For *cis*-**5a** and *cis*-**5d**, these protons were shifted significantly upfield due to the interaction with the fluorenyl ring folded towards cyclohexane. In case of **b** proton, geminal to the triazole ring, the change in chemical shift was over 2 ppm. In *trans*-**5a** and **5d** the **B** protons displayed chemical shifts similar to those in spirooxazolidines **4**. Another noticeable feature resulting from the interaction with fluorenyl ring current is the low chemical shift for triazole proton **a** in *cis*-**5a**. Less effective interaction with the fluorenyl ring current makes this feature less pronounced in *cis*-**5d**. In the oxazolidine fragment, one of the **d** protons in both diastereoisomers becomes positioned above the triazole ring, which reflects in a large diastereotopic shift whereas the differences between **c** protons become smaller. The chemical shift of the fluorenyl proton **m** remains the same for both diastereoisomers, whereas **I** protons display slight diastereotopicity for *trans*-**5a** and *trans*-**5d**, where one of them can be positioned above the triazole ring.

NOESY spectra: possible *cis*-*trans* dimerization

The NOESY spectra recorded for the fmoc-spirooxazolidines **5a-d** suggest that the compounds may form noncovalent dimers stable in chloroform and acetonitrile solutions. The NOESY spectrum

recorded for **5a** in chloroform-d is shown in Figure 7 and a complete set of NOESY spectra recorded for **5a-d** in chloroform-d, as well as NOESY spectrum recorded for **5a** in acetonitrile-d₃ are presented in the Supplementary Information. The key feature pointing towards dimerization, is the presence of NOESY signals between protons previously assigned to different diastereoisomers using the HSQC spectra. These are the triazole proton **a** and the cyclohexyl proton **b**. There are several more signals that could result from dimer formation, but due to the complexity of the spectra, it is difficult to trace them back to particular protons in the structure. In contrast, for the unsubstituted spirooxazolidine **4a**, the NOESY spectrum did not reveal any signals that could be directly attributed to a similar supramolecular complex.

Formation of stable dimers or multimers of fmoc derivatives **5** could partially explain the discrepancies between the experimental ¹H NMR spectra recorded for compound **5a** and the ones computed for its *cis* and *trans* diastereoisomers. It may also provide a chemical rationale for the failure to separate the *cis/trans* diastereoisomeric mixtures through column chromatography.

Initial computational studies aimed at determining the structure of such a complex showed that it is possible to form energetically favourable complexes (see Figure 7). However, finding the actual conformation of the complex would require more sophisticated computational studies, enabling to investigate a large number of potential complex topologies and their respective conformations. Based on the dimer model presented herein and the conformational analysis of the *cis* and *trans* monomers discussed above, it can be hypothesized that an additional interaction to make the complex stable, could be formed by the interaction of the *cis* isomer with the fmoc fragment of *trans*, which displays significant conformational freedom and is unhindered in the complex model. Despite the questions about detailed structure and conformation of the *cis-trans* complex remaining open, the ability of fmoc-spirooxazolidines to spontaneously form *cis-trans* dimers is a noteworthy property and an interesting starting point for further research.

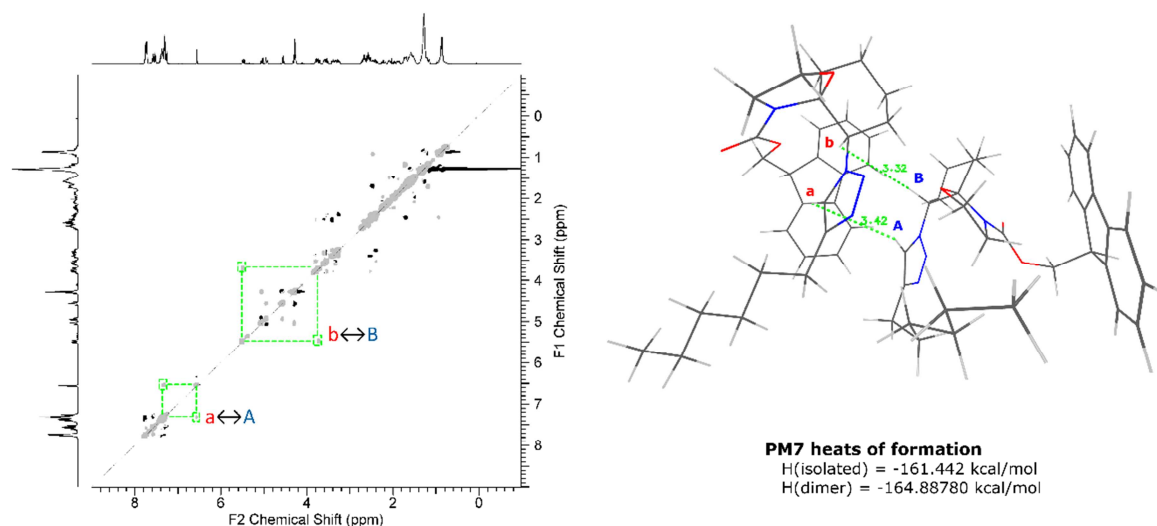


Figure 6 Left: NOESY spectrum of fmoc-oxazolidine **5a**, with *cis-trans* signals marked. Right: A PM7-optimized potential structure of the *cis-trans* **5a** complex with respective distances marked.

UV-VIS absorption and fluorescence spectra

For the obtained diastereoisomeric mixtures of fmoc derivatives **5 a-d**, UV-VIS absorption and fluorescence spectra were recorded; they are shown in figure 7, together with the spectra of fmoc-chloride and propargyl-fmoc⁴¹ as reference. This allowed to evaluate the changes in spectral properties of the fluorenyl chromophore upon attachment to the spirooxazolidine systems, and determine whether the complex formation suggested by NOESY spectra would produce any changes. The absorption and emission spectra recorded for **5a-d** are shown in figure 1, together with the spectra of fmoc-chloride

and propargyl-fmoc⁴¹ as reference. The absorption spectra (Figure 6, top panel) displayed a set of maxima characteristic for the fluorenyl chromophore and similar absorbance intensity, with an exception of compound **5d** which displayed strong absorbance at 255 nm, a characteristic feature of the 4-phenyltriazolyl fragment. The emission spectra, shown in Figure 6 (bottom panel) display no significant changes in shape or position of the maxima, while the intensity for the recorded fluorescence was similar among the compounds investigated. These results could indicate that there is no significant interaction between the fluorenyl chromophores in the *cis-trans* complex as no notable changes in the spectra are observed in comparison to fmoc-chloride and fmoc propargyl ester, for which no evidence of complex formation is present.

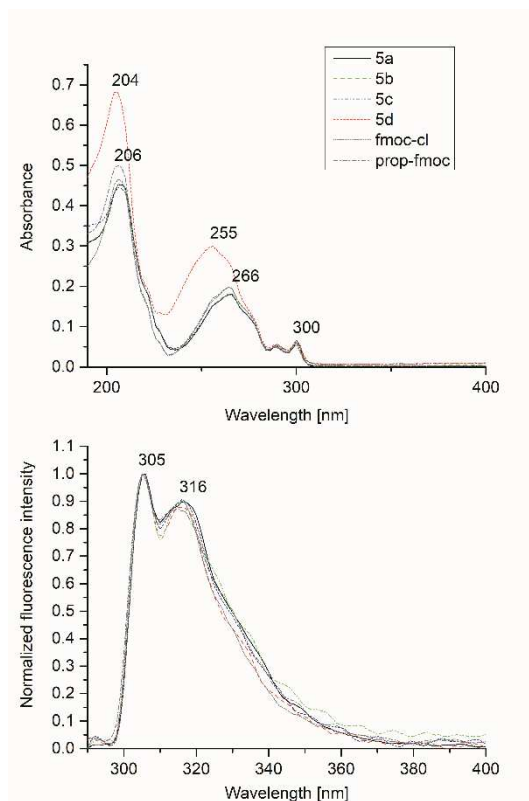


Figure 7. Absorption (top panel) and emission spectra (bottom panel) for **5a-d**

Experimental section

General information

All starting materials were purchased from Sigma-Aldrich and used without further purification. Solvents were purchased from ChemPur. The ¹H NMR (300 MHz), ¹³C NMR (75 MHz) and 2D NMR (COSY, HSQC) spectra were taken in CDCl₃ on a Varian Mercury spectrometer; NOESY spectra and other spectra in acetonitrile d₃ were recorded on a 500 MHz JEOL JNM-ECZR500 RS1 spectrometer. Liquid chromatography-mass spectrometry (LC-MS) analysis was taken on an Acquity TQD apparatus (Waters), equipped with an Acquity UPLC BEH C18 1.7 μm 2.1 x 100 mm column, eluting with 0.3 mL/min of water-acetonitrile mixture containing 0.1% of HCOOH, in 5-100% acetonitrile gradient over 10 min, followed by 2 min of 100% acetonitrile (also containing 0.1% HCOOH). The detection was carried out by e(λ) DAD (diode array detector) and ESI-MS. Elemental analyses were performed using a Vario EL III elemental analyzer (Elementar Analysensysteme GmbH).

Synthetic procedures and spectral data

trans-2-azidocyclohexanol (1). Sodium azide (8.3 g, 127,7 mmol) was dissolved in a mixture of water and acetone (ratio 1:1, 100 mL) at 70°C and the solution was treated with cyclohexene oxide (5.3 mL, 52,4 mmol). After 2.5 h the reaction was completed. The acetone was evaporated under reduced pressure and the residue was extracted with dichloromethane (3 x 20 mL). The extract was washed with water (2 x 10 mL), dried over anhydrous magnesium sulfate and concentrated under reduced pressure to give 6.73 g (94%) of **1** as colorless oil. ¹H NMR (300 MHz, CDCl₃): δ 1.20 – 1.39 (m, 4H), 1.68 – 1.82 (m, 2H), 1.97 – 2.10 (m, 2H), 2.36 (s, 1H), 3.19 (ddd, 1H, *J* = 11 Hz, 9.5 Hz and 4.2 Hz), 3.35 – 3.42 (m, 1H). ¹H NMR matches literature.²⁸

triazolyl cyclohexanols (2a-2d) A solution of 2-azidocyclohexanol (**1**, 1 g, 8,0 mmol) in ethanol (8 mL) was stirred vigorously and treated with an alkyne (8,4 mmol), followed by CuSO₄ (0.05 mol/L, 0.5-5 mol%), 2-{4-[(dimethylamino)methyl]-1,2,3-triazol-1-yl}-cyclohexan-1-ol²⁹ (AMTC, 1-10 mol%) and water (16 mL). The reaction was initiated by addition of sodium ascorbate solution (0.5-5 mol%) and proceeded overnight at 30°C under vigorous stirring. Then the mixture was diluted with aqueous solution of EDTA (5 mL, 2 mg/mL) and extracted with dichloromethane (3 x 20 mL). The extract was washed with aqueous EDTA (15 mL) and water (15 mL) and dried over anhydrous MgSO₄. Concentration under reduced pressure yielded a triazole **2a-2d** as white to pale yellow solid. Crude product **2a-2d** thus obtained was used in the subsequent transformation, as described below, without further purification.

trans-2-(4-Hexyl-1H-1,2,3-triazol-1-yl)cyclohexan-1-ol (2a) Conditions: 5mol% CuSO₄, 10mol% AMTC, 5mol% sodium ascorbate; yield 83%; UPLC-UV purity 97.54% (DAD); LC-MS (ESI): *m/z* calcd for C₁₄H₂₅N₃O (M+H)⁺ 252.21, found 252.27; ¹H NMR (300 MHz, CDCl₃): δ 7.32 (s, 1H), 3.95-4.16 (m, 2H), 2.63-2.68 (t, 2H, *J* = 9Hz), 2.19-2.22 (m, 2H), 1.71-1.92 (m, 3H), 1.59-1.69 (m, 2H), 1.24-1.55 (m, 9H), 0.87-0.91 (t, 3H, *J* = 6Hz). ¹H NMR matches literature.³⁰

trans-2-(4-Heptyl-1H-1,2,3-triazol-1-yl)cyclohexan-1-ol (2b) Conditions: 2mol% CuSO₄, 1mol% AMTC, 2mol% sodium ascorbate; yield 82%. UPLC-UV purity 100.00% (DAD); LC-MS (ESI): *m/z* calcd for C₁₅H₂₇N₃O (M+H)⁺ 266.22, found 266.30; ¹H NMR (300 MHz, CDCl₃): δ 7.30 (s, 1H), 3.95-4.12 (m, 2H), 2.60-2.65 (t, 2H, *J* = 9Hz), 2.13-2.21 (m, 2H), 1.82-1.88 (m, 3H), 1.60-1.67 (m, 2H), 1.24-1.48 (m, 11H), 0.84-0.88 (t, *J* = 6Hz, 3H). ¹H NMR matches literature.³⁰

trans-2-(4-Dodecyl-1H-1,2,3-triazol-1-yl)cyclohexan-1-ol (2c) Conditions: 1mol% CuSO₄, 0,5mol% AMTC, 1mol% sodium ascorbate; yield 92%. UPLC-UV purity 100.00% (DAD); LC-MS (ESI): *m/z* calcd for C₂₀H₃₇N₃O (M+H)⁺ 336.30, found 336.41; ¹H NMR (300 MHz, CDCl₃): δ 7.31 (s, 1 H), 4.05 - 4.16 (m, 1 H), 3.93 - 4.04 (m, 1 H), 2.59 - 2.71 (t, *J*=7.6, 2 H), 2.17 (td, *J*=7.03, 2.93 Hz, 4 H), 1.81 - 1.90 (m, 2 H), 1.62 (m, 2 H), 1.15 - 1.32 (m, 20 H), 0.83 - 0.91 (t, *J*=7.0 Hz, 3 H). ¹H NMR matches literature.³⁰

trans-2-(4-Phenyl-1H-1,2,3-triazol-1-yl)cyclohexan-1-ol (2d) Conditions: 1mol% CuSO₄, 1mol% AMTC, 1mol% sodium ascorbate; yield 82%; mp 177°C. UPLC-UV purity 100.00% (DAD); LC-MS (ESI): *m/z* calcd for C₁₄H₁₇N₃O (M+H)⁺ 244.14, found 244.23. ¹H NMR (300 MHz, CDCl₃): δ 7.74 (s, 1H), 7.65-7.68 (m, 2H), 7.33-7.39 (m, 3H), 4.04-4.20 (m, 2H), 2.18-2.26 (m, 2H), 1.86-2.05 (m, 3H), 1.41-1.52 (m, 3H). ¹H NMR matches literature.⁴²

triazolyl cyclohexanones (3a-3d) A solution of alcohol **2** (0.38 mmol) in dichloromethane (4 mL) was cooled to 3°C and after 5 minutes treated with 0.47 mmol DMP (1.4 eq) dissolved in 3 ml DCM. The reaction mixture was vigorously stirred for 30 minutes at 3°C and left to warm to room temperature. After 4 h reaction time, TLC analyses showed complete conversion of the alcohol. Then, the reaction was quenched with aqueous Na₂S₂O₃ (10 ml), diluted to 50 ml with DCM and washed (3x 10 ml) with aqueous solution of NaHCO₃ and water. The extract was dried over anhydrous MgSO₄ and concentrated under reduced pressure to yield crude product **3a-3d**. Optionally, to remove any

remaining DMP, the crude product could be dissolved in 1:1 ethyl acetate: DCM mixture and filtered through a short pad of silica gel.

2-(4-Hexyl-1H-1,2,3-triazol-1-yl)cyclohexan-1-one (3a) Yield >95%; mp 68°C; UPLC-UV purity 94.81% (DAD); LC-MS (ESI): m/z calcd for C₁₄H₂₃N₃O (M+H)⁺ 250.19, found 250.28; ¹H NMR (300 MHz, CDCl₃): δ 7.33 (s, 1 H), 5.38 (dd, *J* = 12.9 Hz and 5.3 Hz, 1 H), 2.69 - 2.77 (t, *J* = 8.21 Hz, 2 H), 2.52 - 2.63 (m, 2 H), 2.16 - 2.27 (m, 2 H), 2.05 - 2.14 (m, 2 H), 1.76 - 2.00 (m, 2 H), 1.60 - 1.74 (m, 2 H), 1.21 - 1.46 (m, 6 H), 0.87 (t, *J* = 7.03 Hz, 3 H). ¹³C NMR (75 MHz, CDCl₃): δ 203.2, 148.3, 120.5, 67.5, 41.2, 35.0, 31.6, 29.3, 28.9, 27.2, 25.8, 24.6, 22.5, 14.1. Anal. Calcd for C₁₄H₂₃N₃O·0.5H₂O: C, 65.08; H, 9.36; N, 16.26. Found: C, 65.38; H, 10.24; N, 16.85.

2-(4-Heptyl-1H-1,2,3-triazol-1-yl)cyclohexan-1-one (3b) Yield >95%; mp 54°C; UPLC-UV purity 100.00% (DAD); LC-MS (ESI): m/z calcd for C₁₅H₂₅N₃O (M+H)⁺ 264.21, found 264.24; ¹H NMR (300 MHz, CDCl₃): δ 7.33 (s, 1 H), 5.38 (dd, *J* = 12.9, 5.3 Hz, 1 H), 2.68 - 2.78 (t, *J* = 7.62 Hz, 2 H), 2.44 - 2.65 (m, 3 H), 2.05 - 2.27 (m, 3 H), 1.74 - 1.99 (m, 2 H), 1.61 - 1.73 (m, 2 H), 1.18 - 1.45 (m, 8 H), 0.81 - 0.92 ppm (t, *J* = 7.03 Hz, 3 H). ¹³C NMR (75 MHz, CDCl₃): δ 203.3, 148.3, 120.5, 67.5, 41.2, 35.0, 31.7, 29.3, 29.2, 29.0, 27.2, 25.8, 24.6, 22.6, 14.1 ppm. Anal. Calcd for C₁₅H₂₅N₃O: C, 68.40%; H, 9.57%; N, 15.95%. Found: C, 68.19%; H, 13.40%; N, 15.92%.

2-(4-Dodecyl-1H-1,2,3-triazol-1-yl)cyclohexan-1-one (3c) Yield >95%; mp 80°C; UPLC-UV purity 100.00% (DAD); LC-MS (ESI): m/z calcd for C₂₀H₃₅N₃O (M+H)⁺ 334.29, found 334.35; ¹H NMR (300 MHz, CDCl₃): δ 7.32 (s, 1 H), 5.37 (dd, *J* = 13.2, 5.6 Hz, 1 H), 2.68 - 2.77 (t, *J* = 8.21 Hz, 2 H), 2.49 - 2.63 (m, 3 H), 2.05 - 2.28 (m, 3 H), 1.74 - 2.01 (m, 2 H), 1.60 - 1.72 (m, 2 H), 1.20 - 1.42 (m, 18 H), 0.82 - 0.92 ppm (t, *J* = 6.45 Hz, 3 H). ¹³C NMR (75 MHz, CDCl₃): δ 147.8, 120.2, 84.8, 72.5, 68.0, 66.5, 33.6, 31.9, 31.6, 29.3, 29.1, 28.8, 28.5, 25.6, 24.7, 24.2, 24.0, 22.7, 18.4, 14.1 ppm. Anal. Calcd for C₂₀H₃₅N₃O: C, 72.03%; H, 10.58%; N, 12.60%; Found: C, 71.79%; H, 13.81%; N, 12.42%.

2-(4-Phenyl-1H-1,2,3-triazol-1-yl)cyclohexan-1-one (3d) Yield >95%; UPLC-UV purity 99,10% (DAD); LC-MS (ESI): m/z calcd for C₁₄H₁₅N₃O (M+H)⁺ 242.13, found 242.11; ¹H NMR (300 MHz, CDCl₃): δ = 7.78 - 7.92 (m, 3 H), 7.37 - 7.47 (m, 2 H), 7.27 - 7.36 (m, 1 H), 5.45 (dd, *J* = 13.2, 5.6 Hz, 1 H), 2.47 - 2.72 (m, 3 H), 2.07 - 2.29 (m, 3 H), 1.76 - 2.00 ppm (m, 2 H). ¹H NMR matches literature.³³ ¹³C NMR (75 MHz, CDCl₃): δ 203.1, 147.6, 130.6, 128.8, 128.1, 125.7, 119.7, 67.6, 41.3, 35.2, 27.2, 24.5 ppm.

Triazolyl spirooxazolidines (4a-4d) A mixture of triazol-1-ylketone **3a-3d** (0.85 mmol), ethanalamine (5.2 mL, 86 mmol) and anhydrous K₂CO₃ (0.24 g, 1.74 mmol) was heated at 110°C for 1 h, then cooled, diluted with water (5 mL) and extracted with dichloromethane (3 x 20 mL). The extract was washed with water (3 x 10 mL) and concentrated under reduced pressure. The product **4a-4d**, a dull yellow solid, was a diastereoisomeric mixture.

6-(4-Hexyl-1H-1,2,3-triazol-1-yl)-1-oxa-4-azaspiro[4.5]decane (4a) Yield 91%; mp 55°C; UPLC-UV purity 98.26% (DAD); LC-MS (ESI): not observed; ¹H NMR (300 MHz, CDCl₃): δ 7.42 (s, 1 H), 7.37 (s, 1 H), 4.65 (dd, *J* = 12.9, 4.7 Hz, 1 H), 4.40 (dd, *J* = 12.9, 4.1 Hz, 1 H), 3.60 - 3.69 (m, 2 H), 3.09 (dd, *J* = 7.0 Hz, 1 H), 2.79 - 2.95 (m, 2 H), 2.59 - 2.75 (m, 6 H), 2.33 - 2.47 (m, 2 H), 2.02 - 2.18 (m, 4 H), 1.79 - 1.96 (m, 5 H), 1.52 - 1.75 (m, 11 H), 1.18 - 1.40 (m, 12 H), 0.81 - 0.90 ppm (t, *J* = 6.0 Hz, 6 H); ¹³C NMR (75 MHz, CDCl₃): δ 148.2, 147.5, 123.0, 120.3, 96.9, 95.4, 66.3, 65.9, 65.5, 63.8, 45.5, 45.0, 36.8, 31.5, 29.8, 29.7, 29.5, 28.9, 25.7, 25.5, 25.0, 24.8, 23.8, 22.6, 22.4, 14.0; Anal. Calcd for C₁₆H₂₈N₄O: C, 63.75%; H, 9.70%; N, 18.59%. Found: C, 63.96%; H, 10.19%; N, 18.70%.

6-(4-Heptyl-1H-1,2,3-triazol-1-yl)-1-oxa-4-azaspiro[4.5]decane (4b) Yield 99%; mp 47°C; UPLC-UV purity 96.29% (DAD); LC-MS (ESI): not observed; ¹H NMR (300 MHz, CDCl₃): δ 7.42 (s, 1 H), 7.38 (s, 1 H), 4.66 (dd, *J* = 12.9, 4.7 Hz, 1 H), 4.41 (dd, *J* = 13.2, 3.8 Hz, 1 H), 3.56 - 3.73 (m, 2 H), 3.10 (dd, *J* = 7.5 Hz, 1 H), 2.79 - 2.95 (m, 2 H), 2.60 - 2.76 (m, 6 H), 2.34 - 2.47 (m, 2 H), 1.99 - 2.19 (m, 3 H), 1.80 - 1.97 (m, 5 H), 1.51 - 1.78 (m, 11 H), 1.18 - 1.40 (m, 20 H), 0.82 - 0.94 ppm (t,

$J=6.0$ Hz, 6 H); ^{13}C NMR (75 MHz, CDCl_3): δ 148.2, 147.5, 123.0, 120.3, 96.9, 95.4, 66.3, 65.9, 65.5, 63.8, 45.5, 45.0, 36.9, 36.7, 31.8, 29.8, 29.7, 29.5, 29.2, 29.0, 25.7, 25.5, 25.0, 24.8, 23.8, 22.6, 22.4, 14.1 ppm; Anal. Calcd for $\text{C}_{17}\text{H}_{30}\text{N}_4\text{O}$: C, 66.63%; H, 9.87%; N, 18.28%. Found: C, 65.62%; H, 13.68%; N, 17.81%.

6-(4-Dodecyl-1H-1,2,3-triazol-1-yl)-1-oxa-4-azaspiro[4.5]decane (4c) Yield 91%; mp 68°C; UPLC-UV purity 100.00% (DAD); LC-MS (ESI): not observed; ^1H NMR (300 MHz, CDCl_3): δ 7.42 (s, 1 H), 7.37 (s, 1 H), 4.65 (dd, $J=12.6$, 4.4 Hz, 1 H), 4.40 (dd, $J=13.2$, 3.8 Hz, 1 H), 3.58 - 3.70 (m, $J=7.6$ Hz, 2 H), 3.04 - 3.14 (m, $J=6.4$ Hz, 1 H), 2.79 - 2.96 (m, 2 H), 2.59 - 2.74 (m, 6 H), 2.33 - 2.49 (m, 2 H), 1.99 - 2.17 (m, $J=3.5$ Hz, 3 H), 1.78 - 1.96 (m, 5 H), 1.50 - 1.74 (m, 11 H), 1.15 - 1.36 (m, 36 H), 0.86 ppm (t, $J=1.0$ Hz, 6 H); ^{13}C NMR (75 MHz, CDCl_3): δ 148.2, 147.5, 123.0, 120.3, 96.9, 95.4, 66.3, 65.9, 65.5, 63.8, 45.5, 45.0, 36.9, 36.7, 31.9, 29.3, 29.2, 25.7, 25.5, 25.0, 24.8, 23.8, 22.7, 22.4, 14.1 ppm; Anal. Calcd for $\text{C}_{22}\text{H}_{40}\text{N}_4\text{O}$: C, 70.17%; H, 10.71%; N, 14.88%. Found: C, 69.50%; H, 15.66%; N, 14.78%.

6-(4-Phenyl-1H-1,2,3-triazol-1-yl)-1-oxa-4-azaspiro[4.5]decane (4d) Yield 96%; UPLC-UV purity 100% (DAD); LC-MS (ESI): not observed; ^1H NMR (300 MHz, CDCl_3): δ 7.94 (s, 1 H), 7.91 (s, 1 H), 7.85 (m, 4 H), 7.43 (m, 4 H), 7.32 (m, 2 H), 4.75 (dd, $J=12.9$, 4.7 Hz, 1 H), 4.52 (dd, $J=12.9$, 4.1 Hz, 1 H), 3.57 - 3.77 (m, 2 H), 3.21 (dd, $J=7.0$ Hz, 1 H), 2.78 - 3.00 (m, 2 H), 2.67 (dd, $J=10.0$, 4.7 Hz, 1 H), 2.38 - 2.52 (m, 2 H), 2.06 - 2.31 (m, 4 H), 1.83 - 2.01 (m, 4 H), 1.42 - 1.79 ppm (m, 8 H); ^{13}C NMR (75 MHz, CDCl_3): δ 147.5, 146.9, 128.1, 125.6, 121.9, 119.3, 95.4, 66.0, 65.8, 64.2, 45.6, 45.1, 29.8, 22.4 ppm; Anal. Calcd for $\text{C}_{16}\text{H}_{20}\text{N}_4\text{O}$: C, 67.58%; H, 7.09%; N, 19.70%. Found: C, 67.63%; H, 7.41%; N, 18.88%.

N-fluorenylmetoxycarbonyl oxazolidines (5a-5d) To spirooxazolidine 4 (0.42 mmol) and K_2CO_3 (1.3 mmol, 3 eq), 5 mL of dry DCM was added. The mixture was cooled to 0°C. Then, fmoc-Cl (0.44 mmol, 1.05 eq) dissolved in 5 mL DCM was added dropwise over 3 h and the reaction proceeded overnight, slowly warming to room temperature under vigorous stirring. After that, water was added and the mixture was extracted with 3 x 20 mL of DCM. The combined organic layers were washed with 1 x 15 mL of water and dried over anhydrous MgSO_4 . Concentration under reduced pressure yielded the crude product, which was purified by flash chromatography on silica gel eluting with 1:6 ethyl acetate: DCM mixture to obtain product 5a-5d.

(9H-fluoren-9-yl)methyl 6-(4-hexyl-1H-1,2,3-triazol-1-yl)-1-oxa-4-azaspiro[4.5]decane-4-carboxylate (5a) Yield 75%; UPLC-UV purity 96.94% (DAD); LC-MS (ESI): m/z calcd for $\text{C}_{31}\text{H}_{38}\text{N}_4\text{O}_3$ ($\text{M}+\text{H}$)⁺ 515.30, found 515.33; ^1H NMR (300 MHz, CDCl_3): 7.69 - 7.80 (m, 4 H), 7.49 - 7.64 (m, 4 H), 7.27 - 7.44 (m, 9 H), 6.55 (s, 1 H), 5.48 (dd, $J=13.2$, 4.4 Hz, 1 H), 4.85 - 5.15 (m, 2 H), 4.50 - 4.64 (m, 1 H), 4.20 - 4.38 (m, 3 H), 3.75 - 3.85 (m, 1 H), 3.72 (dd, $J=12.9$, 4.1 Hz, 1 H), 3.48 - 3.65 (m, 2 H), 3.41 (ddd, $J=9.4$, 6.4, 2.9 Hz, 1 H), 3.20 - 3.37 (m, 2 H), 2.33 - 2.78 (m, 8 H), 2.03 - 2.28 (m, 3 H), 1.44 - 2.02 (m, 10 H), 1.16 - 1.34 (m, 15 H), 0.82 - 0.93 ppm (m, 8 H); ^1H NMR (500 MHz, CD_3CN): 7.78 - 7.85 (m, 4 H), 7.71 - 7.75 (m, 1 H), 7.63 - 7.66 (m, 1 H), 7.56 - 7.60 (m, 1 H), 7.53 - 7.56 (m, 1 H), 7.44 - 7.48 (m, 1 H), 7.38 - 7.43 (m, 8 H), 7.31 - 7.37 (m, 4 H), 7.25 - 7.30 (m, 2 H), 6.84 (s, 1 H), 5.33 (dd, $J=13.2$, 4.6 Hz, 1 H), 4.91 (d, $J=2.9$ Hz, 2 H), 4.40 - 4.44 (m, 1 H), 4.31 - 4.34 (m, 1 H), 4.22 - 4.29 (m, 1 H), 3.73 - 3.78 (m, 7 H), 3.70 (dd, $J=12.6$, 4.0 Hz, 1 H), 3.55 - 3.60 (m, 1 H), 3.46 - 3.53 (m, 1 H), 3.31 - 3.37 (m, 1 H), 3.24 - 3.29 (m, 1 H), 3.10 - 3.15 (m, 1 H), 2.56 - 2.67 (m, 2 H), 2.49 - 2.55 (m, 2 H), 2.31 - 2.40 (m, 1 H), 1.45 - 1.73 (m, 9 H), 1.41 (dd, $J=8.6$, 4.0 Hz, 1 H), 1.26 (br. s., 12 H), 1.09 - 1.15 (m, 2 H), 0.84 ppm (d, $J=7.4$ Hz, 6 H); ^{13}C NMR (75 MHz, CDCl_3): 152.6, 152.1, 147.2, 144.3, 144.0, 143.5, 141.2, 127.8, 127.6, 127.5, 127.4, 127.1, 127.0, 125.2, 125.0, 124.6, 124.1, 120.4, 120.0, 119.9, 94.5, 93.8, 67.2, 65.7, 64.1, 63.3, 60.8, 60.2, 47.2, 45.6, 45.2, 41.2, 35.0, 32.6, 31.6, 29.6, 29.3, 29.1, 28.9, 28.6, 27.2, 25.8, 25.7, 25.5, 24.6, 24.3, 23.5, 22.6, 22.4, 22.0, 14.1 ppm; Anal. Calcd for $\text{C}_{31}\text{H}_{38}\text{N}_4\text{O}_3 \cdot 0.5\text{H}_2\text{O}$: C, 71.10%; H, 7.51%; N, 10.70%. Found: C, 70.85%; H, 6.46%; N, 10.88%.

(9H-fluoren-9-yl)methyl 6-(4-heptyl-1H-1,2,3-triazol-1-yl)-1-oxa-4-azaspiro[4.5]decane-4-carboxylate (5b) Yield 72%; UPLC-UV purity 98.66% (DAD); LC-MS (ESI): *m/z* calcd for C₃₂H₄₀N₄O₃ (M+H)⁺ 529.32, found 529.36; ¹H NMR (300 MHz, CDCl₃): 7.70 - 7.78 (m, 4 H), 7.48 - 7.63 (m, 4 H), 7.27 - 7.45 (m, 9 H), 6.55 (s, 1 H), 5.48 (dd, *J*=13.2, 4.4 Hz, 1 H), 4.89 - 5.09 (m, 2 H), 4.50 - 4.62 (m, 1 H), 4.22 - 4.34 (m, 3 H), 3.75 - 3.85 (m, 1 H), 3.72 (dd, *J*=12.9, 4.1 Hz, 1 H), 3.48 - 3.65 (m, 2 H), 3.41 (ddd, *J*=9.7, 6.4, 3.2 Hz, 1 H), 3.20 - 3.37 (m, 2 H), 2.35 - 2.75 (m, 8 H), 2.03 - 2.32 (m, 3 H), 1.46 - 2.01 (m, 10 H), 1.16 - 1.35 (m, 19 H), 0.77 - 0.99 ppm (m, 8 H); ¹³C NMR (75 MHz, CDCl₃): 152.6, 152.1, 147.2, 146.7, 144.3, 144.0, 143.5, 141.4, 141.3, 141.2, 127.8, 127.7, 127.6, 127.1, 127.0, 125.2, 125.0, 124.6, 124.1, 120.5, 119.9, 94.5, 93.8, 67.2, 65.7, 64.1, 63.3, 60.9, 60.3, 47.2, 45.6, 45.2, 41.2, 35.0, 32.6, 31.8, 29.6, 29.2, 29.0, 28.5, 27.2, 25.6, 25.5, 24.6, 24.3, 23.4, 22.7, 22.6, 22.4, 22.0, 14.1 ppm; Anal. Calcd for C₃₂H₄₀N₄O₃·0.5H₂O: C, 72.70%; H, 7.63%; N, 10.60%. Found: C, 71.92%; H, 9.10%; N, 10.80%.

(9H-fluoren-9-yl)methyl 6-(4-dodecyl-1H-1,2,3-triazol-1-yl)-1-oxa-4-azaspiro[4.5]decane-4-carboxylate (5c) Yield 70%; UPLC-UV purity 99.22% (DAD); LC-MS (ESI): *m/z* calcd for C₃₇H₅₀N₄O₃ (M+H)⁺ 599.40, found 599.22; ¹H NMR (300 MHz, CDCl₃): 7.71 - 7.78 (m, 4 H), 7.49 - 7.63 (m, 4 H), 7.27 - 7.44 (m, 9 H), 6.55 (s, 1 H), 5.48 (dd, *J*=12.9, 4.1 Hz, 1 H), 4.88 - 5.10 (m, 2 H), 4.50 - 4.63 (m, 1 H), 4.28 (d, *J*=5.9 Hz, 3 H), 3.75 - 3.84 (m, 1 H), 3.72 (dd, *J*=12.9, 4.1 Hz, 1 H), 3.49 - 3.65 (m, 2 H), 3.40 (d, *J*=2.9 Hz, 1 H), 3.21 - 3.36 (m, 2 H), 2.34 - 2.75 (m, 8 H), 2.02 - 2.32 (m, 3 H), 1.43 - 2.01 (m, 10 H), 1.15 - 1.34 (m, 40 H), 0.76 - 0.94 ppm (m, 8 H); ¹³C NMR (75 MHz, CDCl₃): 152.6, 152.1, 147.2, 146.8, 144.3, 144.0, 143.5, 141.4, 141.2, 127.8, 127.6, 127.1, 125.2, 125.0, 124.7, 124.1, 120.5, 94.5, 93.8, 67.2, 65.7, 64.1, 63.3, 60.8, 60.3, 47.2, 45.6, 45.2, 41.2, 35.1, 32.6, 31.9, 29.6, 29.4, 29.2, 29.0, 28.6, 25.7, 25.5, 24.3, 23.4, 22.7, 22.4, 22.0, 14.1 ppm; Anal. Calcd for C₃₇H₅₀N₄O₃·0.5H₂O: C, 73.11%; H, 8.46%; N, 9.22%. Found: C, 72.61%; H, 9.17%; N, 9.62%.

(9H-fluoren-9-yl)methyl 6-(4-phenyl-1H-1,2,3-triazol-1-yl)-1-oxa-4-azaspiro[4.5]decane-4-carboxylate (5d) Yield 76%; UPLC-UV purity 100.0% (DAD); LC-MS (ESI): *m/z* calcd for C₃₁H₃₀N₄O₃ (M+H)⁺ 507.24, found 507.16; ¹H NMR (300 MHz, CDCl₃): 7.87 (s, 1 H), 7.71 - 7.85 (m, 9 H), 7.58 (td, *J*=11.4, 7.6 Hz, 3 H), 7.27 - 7.48 (m, 14 H), 7.21 (s, 1 H), 5.62 (dd, *J*=13.2, 4.4 Hz, 1 H), 4.96 - 5.11 (m, 2 H), 4.54 - 4.66 (m, 1 H), 4.26 - 4.35 (m, 3 H), 3.76 - 3.90 (m, 2 H), 3.69 (td, *J*=7.6, 2.9 Hz, 1 H), 3.51 - 3.62 (m, 1 H), 3.37 - 3.47 (m, 2 H), 3.28 (ddd, *J*=9.8, 6.6, 2.9 Hz, 1 H), 2.59 (td, *J*=9.4, 7.0 Hz, 1 H), 2.39 - 2.53 (m, 3 H), 2.11 - 2.35 (m, 3 H), 1.54 - 2.03 (m, 7 H), 1.20 - 1.37 (m, 3 H), 0.83 - 0.98 ppm (m, 2 H); ¹³C NMR (75 MHz, CDCl₃): 152.6, 152.2, 146.6, 146.2, 144.3, 144.1, 143.6, 141.4, 141.4, 141.2, 130.9, 130.8, 128.8, 128.7, 128.0, 127.9, 127.8, 127.7, 127.6, 127.6, 127.4, 127.1, 127.0, 125.6, 125.3, 125.0, 124.8, 124.2, 120.0, 119.9, 119.9, 119.5, 119.3, 94.5, 93.7, 67.3, 65.8, 64.2, 63.4, 61.0, 60.5, 47.2, 47.2, 45.6, 45.3, 32.4, 32.4, 29.2, 28.7, 24.3, 23.4, 22.4, 22.0 ppm

Computational procedure

The applied procedure is in principle analogous to the one described by Willoughby⁴³, with slight modifications and different software packages used. First, a large set of conformations for each investigated diastereoisomer was generated: over 100 conformations for **4a** and 250-300 conformations for **5a** and **5d**. This task was completed using the Balloon conformational search program, which employs the MMFF94 force field for energy evaluation and a genetic algorithm approach for structure evolution and selection.^{35,44} For the conformational searches, *n*=100 starting conformations were created from scratch and the algorithm was allowed to evolve over 1000 000 generations. Thus generated structures were optimized using the PM7 semiempirical quantum chemistry method,³⁷ as implemented in MOPAC 2016,³⁸ using the COSMO solvent model for chloroform (approx. molecular radius of 2.5 Å and dielectric constant of 4.81 were taken). For **4a**, 10 conformations displaying the lowest heats of formation were taken for DFT-based optimization, while

conformation number was increased to 20. The selected conformations were then optimized using the widely-applied B3LYP correlation-exchange functional, 6-31G(d,p) basis set and IEFPCM model for chloroform, as implemented in the Gaussian09 package.³⁹ After optimization, frequencies and thermochemical data were calculated and thus computed total free energies of formation were used to compute Boltzmann distribution. The conformations generated in all the steps are depicted in Figures S1 (**cis** and **trans 4a**), S2 (**cis** and **trans 5a**) and S3 (**cis** and **trans 5d**) in Supplementary Information. The graphical representations were generated using VMD.⁴⁵ For the conformations taken for NMR calculation, coordinates and isotropic shielding constants are given in Supplementary Information.

For shielding constant calculation the GIAO method was employed, as a method of choice for this type of calculations.^{43,46} The DFT GIAO computations were performed using the CAMB3LYP functional, cc-pvtz basis set and IEFPCM solvent model for chloroform, as implemented in Gaussian09, the computation was performed for the conformations making up over 95% of the total Boltzmann occupancy. Chemical shifts were calculated using the formula below, using tetramethylsilane as chemical shift reference.

$$\delta_i = \sigma_{TMS} - \frac{\sum_j b_j \cdot \sigma_{ij}}{\sum_j b_j}$$

δ_i is the chemical shift of *i*-th atom, b_j and σ_{ij} are Boltzmann occupancy for conformer *j* and isotropic shielding constant for *i*-th proton in this conformer, σ_{TMS} is the isotropic shielding constant for tetramethylsilane (TMS) main text of the article should appear here with headings as appropriate.

The potential dimer structures were constructed from the B3LYP-optimized geometries of **cis**- and **trans- 5a**. For **trans-5a**, both possible enantiomers were considered by generating mirror images of the previously considered conformations. In this way, it was possible to consider the possible diastereoisomeric complexes. The complexes were built using a simple evolutionary algorithm developed for that purpose. The algorithm was designed to find rotation and translation parameters to bring selected protons in the structures into close contact (2 Å distance), avoiding other contacts closer than 1.9Å. This was achieved by alternating two fitness functions, the first one promotes the “desired” contacts, while the other, optimized to avoid the “undesired” ones”. The conformations taken for complex construction were kept unchanged by the algorithm, only rotation and translation parameters were modified. From the thus generated >700 complexes, the ones where the distances between the selected protons were smaller than 3Å were chosen for PM7-level optimization with Mopac 2016. The obtained heats of formation were compared to the best conformations of isolated **cis** and **trans-5a**.

Conclusions

The developed synthetic route allowed to quickly build complex molecular structures of novel triazolyl spirooxazolidines **4** and their fmoc derivatives **5**. Overall yields of the synthesis were good: 68-75% over 4 steps for **4a-d** and 51-53% over 5 steps for **5a-d**. The combination of computational studies with experimental NMR measurements allowed to assign ¹H NMR signals to respective diastereoisomers as well as to understand the conformational dynamics of the compounds and the influence of aromatic ring currents. Moreover, the performed studies revealed that the obtained fmoc-oxazolidines may form stable noncovalent **cis-trans** dimers. The measured absorption and emission spectra showed no significant changes compared to the “mother” fluorenyl chromophore.

Conflicts of interest

There are no conflicts to declare.

Acknowledgements

The computational resources and Gaussian09 E license were provided by Cyfronet AGH within the PL-GRID infrastructure.

References

1. Steemers L, Wanner MJ, Lutz M, Hiemstra H, van Maarseveen JH. *Nat Commun.* 2017; 8: 15392.
2. Bao D-H, Wu H-L, Liu C-L, Xie J-H, Zhou Q-L. *Angew Chemie Int Ed.* 2015; 54: 8791–8794.
3. Huang J-R, Sohail M, Taniguchi T, Monde K, Tanaka F. *Angew Chemie.* 2017; 129: 5947–5951.
4. Kolb HC, Finn MG, Sharpless KB. *Angew Chemie (1 H C Kolb, M G Finn K B Sharpless, Angew Chem Int Ed Engl, 2001, 40, 2004–2021 International ed English).* 2001; 40: 2004–2021.
5. Thirumurugan P, Matosiuk D, Jozwiak K. *Chem Rev.* 2013; 113: 4905–79.
6. Kolb HC, Sharpless KB. *Drug Discov Today.* 2003; 8: 1128–1137.
7. Tron GC, Pirali T, Billington RA, Canonico PL, Sorba G, Genazzani AA. *Med Res Rev.* 2008; 28: 278–308.
8. Lallana E, Sousa-Herves A, Fernandez-Trillo F, Riguera R, Fernandez-Megia E. *Pharm Res.* 2012; 29: 1–34.
9. Binder WH, Sachsenhofer R. *Macromol Rapid Commun.* 2007; 28: 15–54.
10. Binder W, Sachsenhofer R. *Macromol Rapid Commun.* 2008; 29: 952–981.
11. Johnson JA, Koberstein JT, Turro NJ, Johnson JA, Finn M. *Macromol Rapid Commun.* 2008; 29: 1052–1072.
12. Rostovtsev V V., Green LG, Fokin V V., Sharpless KB. *Angew Chemie - Int Ed.* 2002; 41: 2596–2599.
13. Cope AC, Hancock EM. *J Am Chem Soc.* 1942; 64: 1503–1506.
14. Hancock EM, Hardy EM, Heyl D, Wright ME, Cope AC. *J Am Chem Soc.* 1944; 66: 1747–1752.
15. Guerrero-Alvarez JA, Moncayo-Bautista A, Ariza-Castolo A. *Magn Reson Chem.* 2004; 42: 524–533.
16. Faidallah HM, Sharshira EM, AL-Saadi MSM. *Heterocycl Commun.* 2009; 15: 43–50.
17. Ye F, Fu Y, Kang J-X, Wang Y-K, Liu J, Zhao L-X, Gao S. *Heterocycles.* 2016; 92: 740.
18. De Petrocellis L, Cascio MG, Di Marzo V. *Br J Pharmacol.* 2004; 141: 765–74.
19. Petrosino S, Iuvone T, Di Marzo V. *Biochimie.* 2010; 92: 724–727.
20. Di Marzo V, Bifulco M, De Petrocellis L. *Nat Rev Drug Discov.* 2004; 3: 771–84.
21. Pertwee RG. *Br J Pharmacol.* 2006; 147 Suppl: S163-71.
22. Yamada K, Hirabayashi J, Kakehi K. *Anal Chem.* 2013; 85: 3325–3333.
23. Báez ME, Fuentes E, Espina MJ, Espinoza J. *J Sep Sci.* 2014; 37: 3125–3132.
24. Mohammadi B, Majnooni MB, Khatabi PM, Jalili R, Bahrami G. *J Chromatogr B.* 2012; 880: 12–18.
25. Tao K, Levin A, Adler-Abramovich L, Gazit E. *Chem Soc Rev.* 2016; 45: 3935–3953.
26. Tanifuji R, Koketsu K, Takakura M, Asano R, Minami A, Oikawa H, Oguri H. *J Am Chem*

- Soc.* 2018; 140: 10705–10709.
27. Lypson AB, Wilcox CS. *J Org Chem.* 2017; 82: 898–909.
 28. Schramm H, Christoffers J. *Tetrahedron Asymmetry.* 2009; 20: 2724–2727.
 29. Szafranski PW, Kasza P, Cegła MT. *Tetrahedron Lett.* 2015; 56: 6244–6247.
 30. Szafranski PW, Dyduch K, Kosciolatek T, Wróbel TP, Gómez-Cañas M, Gómez-Ruiz M, Fernandez-Ruiz J, Mlynarski J, W. Szafranski P, Dyduch K, Kosciolatek T, P. Wrobel T, Gomez-Canas M, Gomez-Ruiz M, Fernandez-Ruiz J, Mlynarski J. *Lett Drug Des Discov.* 2013; 10: 169–172.
 31. Albadi J, Keshavarz M. *Synth Commun.* 2013; 43: 2019–2030.
 32. Albadi J, Keshavarz M, Shirini F, Vafaie-nezhad M. *Catal Commun.* 2012; 27: 17–20.
 33. Kumar D, Reddy VB, Varma RS. *Tetrahedron Lett.* 2009; 50: 2065–2068.
 34. Vyas VK, Bhanage BM. *Org Lett.* 2016; 18: 6436–6439.
 35. Vainio MJ, Johnson MS, And MJV, Johnson MS. *J Chem Inf Model.* 2007; 47: 2462–2474.
 36. Santeri PJ, J. VM, S. JM. *J Comput Chem.* 2009; 31: 1722–1732.
 37. Stewart JJP. *J Mol Model.* 2013; 19: 1–32.
 38. Stewart JJP. 2016.
 39. M. J. Frisch, G. W. Trucks, H. B. Schlegel GES, M. A. Robb, J. R. Cheeseman, G. Scalmani, V. Barone BM, G. A. Petersson, H. Nakatsuji, M. Caricato, X. Li HPH, A. F. Izmaylov, J. Bloino, G. Zheng, J. L. Sonnenberg MH, M. Ehara, K. Toyota, R. Fukuda, J. Hasegawa, M. Ishida TN, Y. Honda, O. Kitao, H. Nakai, T. Vreven, J. A. Montgomery J, J. E. Peralta, F. Ogliaro, M. Bearpark, J. J. Heyd EB, K. N. Kudin, V. N. Staroverov, T. Keith, R. Kobayashi JN, K. Raghavachari, A. Rendell, J. C. Burant, S. S. Iyengar JT, M. Cossi, N. Rega, J. M. Millam, M. Klene, J. E. Knox JBC, V. Bakken, C. Adamo, J. Jaramillo, R. Gomperts RES, O. Yazyev, A. J. Austin, R. Cammi, C. Pomelli JWO, R. L. Martin, K. Morokuma, V. G. Zakrzewski GAV, P. Salvador, J. J. Dannenberg, S. Dapprich ADD, Farkas O, J. B. Foresman JVO, Cioslowski J, Fox DJ. *Gaussian 09, Revis. E.01*, 2013.
 40. Tomasi J, Mennucci B, Cammi R. *Chem Rev.* 2005; 105: 2999–3094.
 41. Szafranski PW, Kasza P, Kępczyński M, Cegła MT. *Heterocycl Commun.* 2015; 21: 263–267.
 42. Chassaing S, Sido ASS, Alix A, Kumarraja M, Pale P, Sommer J. *Chem - A Eur J.* 2008; 14: 6713–6721.
 43. Willoughby PH, Jansma MJ, Hoyer TR. *Nat Protoc.* 2014; 9: 643–660.
 44. Puranen JS, Vainio MJ, Johnson MS. *J Comput Chem.* 2010; 31: 1722–1732.
 45. Humphrey W, Dalke A, Schulten K. *J Mol Graph.* 1996; 14: 33–38.
 46. Lodewyk MW, Siebert MR, Tantillo DJ. *Chem Rev.* 2012; 112: 1839–1862.

Fluorescent triazolyl spirooxazolidines: synthesis and NMR stereochemical studies**Article Highlights**

- An efficient synthetic pathway towards novel spirooxazolidine derivatives
- PM7 semiempirical studies explored large conformational space
- 1D and 2D NMR combined with DFT allowed to explain complex spectra
- UV-VIS absorption and emission spectra were recorded
- NOESY spectra indicated dimer formation